(Invited) Mid-Infrared Colloidal Quantum Dot Based Nanoelectronics and Nano-Optoelectronics

ECS Transactions, 92 (1) 11-16 (2019)
10.1149/09201.0011ecst ©The Electrochemical Society

Mid-Infrared Colloidal Quantum Dot Based Nanoelectronics and Nano-optoelectronics

Shihab B. Hafiz[a], Michael R. Scimeca[b], Ayaskanta Sahu[b], Dong-Kyun Ko[a]

[a] Department of Electrical and Computer Engineering, New Jersey Institute of Technology, Newark, New Jersey 07102, USA
[b] Department of Chemical and Biomolecular Engineering, New York University, Brooklyn, New York 11201, USA

Electronic and optoelectronic devices fabricated from colloidal quantum dots (CQDs) provide a promising path toward realizing low-cost devices with greatly simplified device fabrication procedure, owing to their solution-processability. The impact that CQD technology would bring is expected to be significant, especially in the mid-infrared application areas, which is currently dominated by epitaxial semiconductor technologies. In this work, we introduce a new generation of infrared CQDs, namely Ag_2Se CQDs, which has been recently uncovered to show distinct optical absorption in the mid-infrared. We report on the fabrication of solution-processed photoconductive photodetectors and discuss our analyses on the electronic and optoelectronic characteristics of our devices. We also demonstrate the feasibility of mid-infrared photodetection with a measured peak responsivity of 0.16 mA/W at 4 μm under room temperature operation.

Introduction

Colloidal suspensions containing single-nanocrystalline semiconductors, or colloidal quantum dots (CQDs), have been a focus of considerable effort in electronic and optoelectronic research for the past fifteen years (1,2). CQDs provide the advantage of low-cost, large-area solution processing, similar to polymers, with desirable physical properties arising from acrystalline semiconductor core. Broad spectral tunability offered by size-dependent quantum confinement has been the major driver in this field. Continuous effort in CQD-based infrared photodetector development has led to a performance that rivals their epitaxial counterparts in the near infrared (NIR, 0.7-1.0 μm) and short-wavelength infrared (SWIR, 1.0-2.5 μm) regimes (3). Specifically, SWIR photodiodes based on PbS CQDs have demonstrated a detectivity of $D^* = 7\times10^{13}$ Jones at room temperature which exceeds the performance of a commercial InGaAs photodetector (4). Moreover, SWIR focal plane arrays (FPAs) have also been fabricated via directly spin-casting CQDs on top of silicon readout integrated circuits (ROICs),(5) without the need of costly hybridization steps (indium bump bonding) required in traditional imaging chip fabrication (6). This combination of high room temperature performance and low-cost manufacturing makes CQD technology uniquely suited to advance the research toward the mid-infrared region where no other solution-processed material options exist. The current leading mid-infrared CQD material is HgTe (7,8) and the toxicity of mercury is expected to be a major limitation for practical applications. An

alternate, non-toxic CQD materials is Ag_2Se, which has been recently discovered to exhibit distinct mid-infrared absorption (9,10). Silver selenide is a member of I-VI semiconductor family that has been rarely used for infrared photodetection. When synthesized into a colloidal nanometer-sized crystal, a new crystal structure (tetragonal) is obtained (11), which is a phase inaccessible in bulk. Tetragonal Ag_2Se is reported to have extremely narrow bandgap of 0.07 eV and the excess in non-stoichiometric silver in CQDs induce n-doping to such an extent that optical transitions occur within the conduction energy levels (intraband transition) (12,13). In this work, we investigate the electronic and optoelectronic characteristics of Ag_2Se CQD devices and demonstrate the feasibility toward mid-infrared photodetector applications.

Experiments

Colloidal Quantum Dot Synthesis and Characterizations

Ag_2Se CQs having average size of 5.5 nm were synthesized using conventional hot-injection technique (9). In brief, 15 mL of oleylamine was added to three-neck reaction flask and degassed at 90 ˚C for 1 hour under vacuum. Meanwhile, 0.5 M silver and 1M selenium precursor solutions were prepared by dissolving silver chloride and selenium powder in triocylphosphine, respectively. After switching to nitrogen environment, 2mL of selenium precursor was first injected into the reaction flask and the temperature was raised to 160 ˚C. Then, 2mL of silver precursor was rapidly injected under vigorous stirring, immediately forming a dark brown solution. The reaction was terminated after 3 seconds of growth, by injecting 10 mL of butanol, followed by cooling via water bath. The CQD products were purified using a mixture of ethanol and methanol and redispersed in a mixture of hexane and octane for thin-film deposition. Standard air-free Schlenk technique was employed throughout the synthesis.

The average size of Ag_2Se CQDs can be controlled from 5.5 to 9.2 nm, with mid-infrared absorption peak varying from 4 to 8 μm, by modifying the injection temperature and growth time (5.5 - 6.5 nm), changing the Ag:Se concentration ratio (6.5 - 8nm), and applying regrowth through additional injection of precursors (> 8 nm). Transmission electron microscopy (TEM) was used to characterize the average size and size dispersion of CQDs. X-ray diffraction (XRD) and energy dispersive X-ray spectroscopy (EDXS) was performed for structural and chemical characterizations, respectively. Infrared optical properties were characterized using Fourier-transform infrared spectroscopy (FTIR).

Device Fabrication and Measurements

Photoconductive photodetectors were fabricated by drop-casting Ag_2Se CQD solution on Si/SiO_x substrates pre-patterned with Cr/Au interdigitated electrodes formed via photolithography. Three to four cycles of CQD film deposition and ligand-exchange (0.1 M 1,2-ethanedithiol in methanol) were repeated to form 70 ± 10 nm thick film. CQD films deposited outside the sensor area were removed to complete the device. Field-effect transistor measurements were performed by depositing Ag_2Se CQDs on heavily p-doped Si/SiO_x substrate and applying gate bias to the substrate. Transfer characteristics were obtained using Agilent 4155A semiconductor parameter analyzer. The spectral

responsivity measurement was performed using calibrated blackbody (900 ˚C) as an infrared radiation source. The source was modulated using an optical chopper and a set of band-pass filters with center wavelength varying from 2-7 μm were used for spectral discrimination. Photocurrents were measured using SR830 lock-in amplifier coupled with SR570 preamplifier. The responsivity was calculated by dividing the photocurrent with optical power estimated for each center wavelength.

Results and Discussion

Figure 1 shows the infrared optical absorption spectra of Ag_2Se CQDs which can be tuned from 4 to 8 μm by varying the CQD size from 5.5 to 9.2 nm. Similar to traditional interband CQDs, the intraband CQDs also exhibit tunable optical properties since the size-dependent quantum confinement controls the intraband transition gap (energy gap between the first and second conduction energy levels).

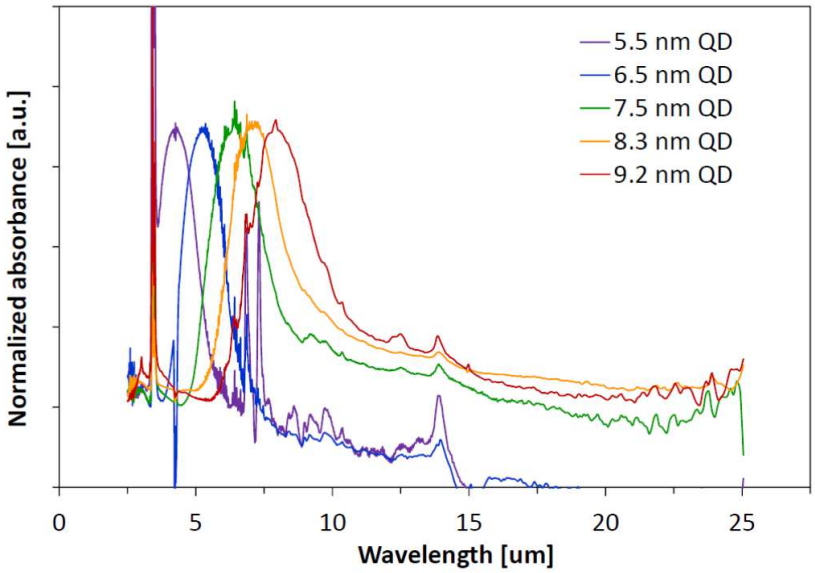

Figure 1. Optical absorption spectra of Ag_2Se CQDs of varying sizes, obtained through FTIR measurements.

Ag_2Se CQDs having average size of 5.5 ± 0.4 nm with optical absorption peak centered at 4 μm, which will be the focus of our device study, is shown in Figure 2. The TEM analysis indicated that CQDs are uniform in size and shape which is in agreement with the sharp absorption features observed in the infrared optical spectra shown in Figure 1. XRD characterization show diffraction peaks that are different from the bulk (orthorhombic) which can be indexed to a tetragonal crystal structure (9,11). The average nanocrystal size estimated from the Scherrer broadening is in agreement with the TEM analysis (~ 5 nm). EDXS analysis confirms that CQDs are composed of Ag and Se. Quantitative analysis estimate Ag:Se ratio of 3.5 – 4, a large excess of stoichiometric Ag, which is responsible for electron-rich character of CQDs.

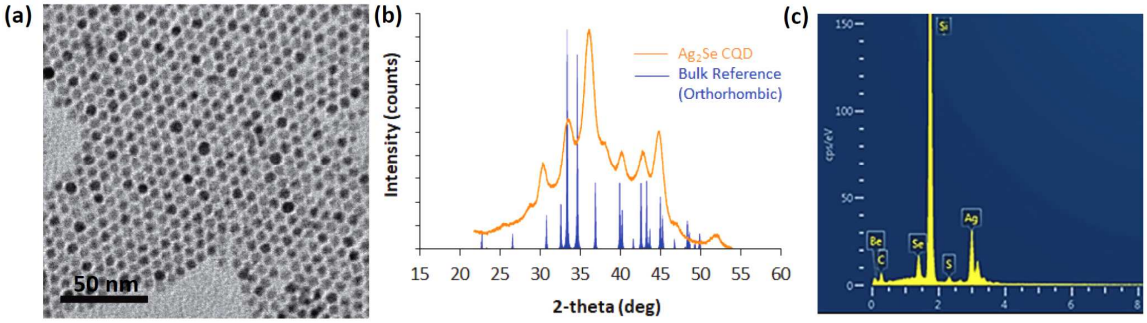

Figure 2. (a) TEM image of as-synthesized Ag_2Se CQDs. (b) and (c) show XRD diffractogram and EDX spectrum obtained from Ag_2Se CQD films.

Field-effect transistor characterization has been widely used in the CQD electronics community to study carrier transport in films composed of CQDs (14). Figure 3 shows the transfer characteristics of a bottom-gate/top-contact field-effect transistor fabricated from Ag_2Se CQD film (ligand exchanged with 1,2-ethanedithiol). The small gate response is an indicative of degenerate doping and higher drain current toward positive gate bias suggest that electrons are the majority carriers; both results are consistent with the material characterizations discussed previously. The gate current is also plotted to confirm that there were negligible leakage currents.

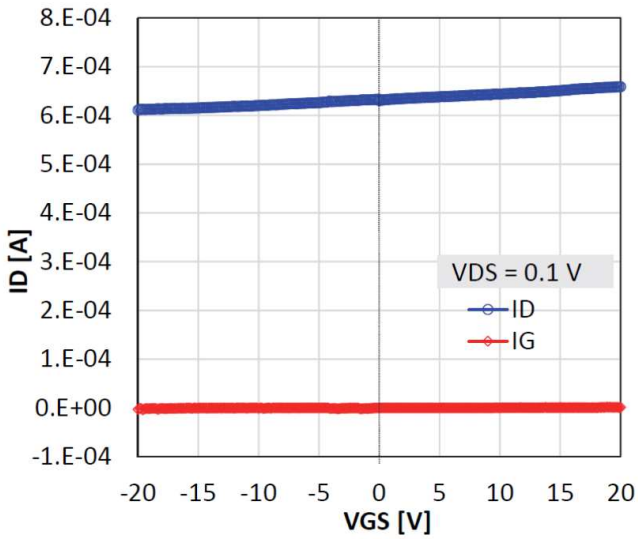

Figure 3. Transfer characteristic of a field-effect transistor fabricated using Ag_2Se CQD film.

Photoconductive photodetectors based on Ag_2Se CQDs were fabricated for spectral responsivity characterization. As the bias was increased up to 0.25 V, a concomitant increase in responsivity with a peak at 4 μm is observed, as shown in Figure 4. Increasing the bias increases the charge separation and collection, which result in an increase in the photocurrent thereby enhancing the responsivity. The spectral shape of the responsivity data coincides with the optical absorption spectrum (obtained from ligand-exchanged

CQD film), indicating that Ag_2Se CQDs are responsible for the observed photoresponse in the mid-infrared. All measurements were performed at room temperature.

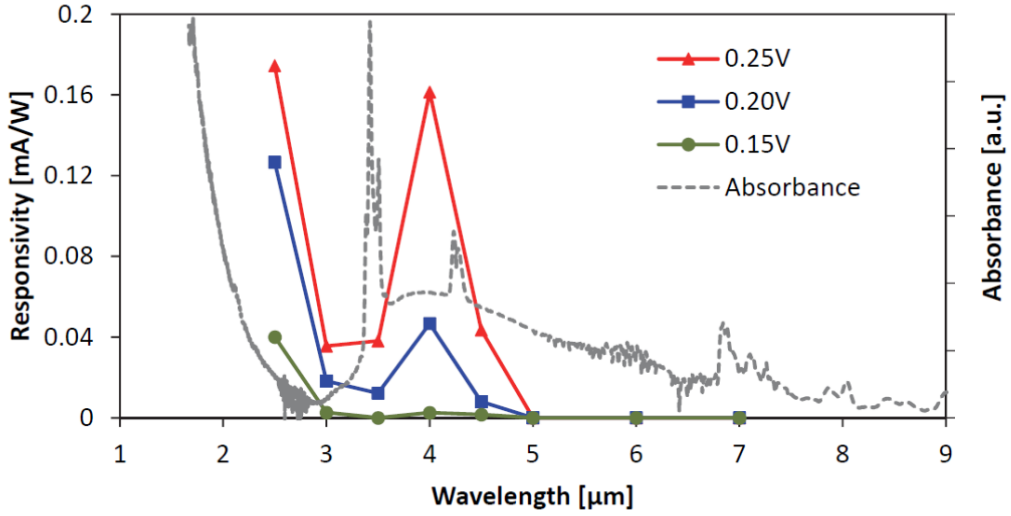

Figure 4. Spectral responsivity of Ag_2Se CQD-based photoconductive photodetector. Optical absorbance spectra of Ag_2Se CQD film (ligand exchanged with 1,2-ethanedithiol) is overlaid for comparison.

Conclusion

Current mid-infrared photodetector technologies suffer from cost and production barriers to wide scale adoption. The room-temperature mid-infrared photodetection demonstrated in this study serves as a necessary groundwork for realizing future low-cost thermal infrared sensors and imagers that may be ubiquitously utilized for various emerging applications. Toward improved detector performance, further efforts are on the way to investigate various types of ligands that have been reported to yield high carrier mobility and surface passivation.

Acknowledgments

This work was supported by the National Science Foundation under Grants ECCS-1809112 (D.K.) and ECCS-1809064 (A.S.).

References

1. C. R. Kagan, E. Lifshitz, E. H. Sargent, and D. V. Talapin, *Science*, **353**, aac5523 (2016).
2. D. V. Talapin, J. –S. Lee, M. V. Kovalenko, and E. V. Shevchenko, *Chem. Rev.*, **110**, 389-458 (2010)
3. R. Saran and R.J. Curry, *Nat. Photonics*, **10**, 81–92 (2016).

4. J. P. Clifford, G. Konstantatos, K. W. Johnston, S. Hoogland, L. Levina, and E. H. Sargent, *Nat. Nanotechnol.,* **4**, 40-44 (2009).
5. E. J. Klem, C. Gregory, D. Temple, and J. Lewis, *Proc. SPIE,* **9451**, 945104 (2015).
6. A. Rogalski, *Rep. Prog. Phys.*, **68**, 2267 (2005).
7. M. M. Ackerman, X. Tang, and P. Guyot-Sionnest, *ACS Nano*, **12**, 7264-7271 (2018)
8. X. Tang, M. M. Ackerman, and P. Guyot-Sionnest, *ACS Nano*, **12**, 7362-7370 (2018).
9. A. Sahu, A. Khare, D. Deng, and D. J. Norris, *Chem. Commun.*, **48**, 5458– 5460 (2012).
10. S. Hafiz, M. R. Scimeca, P. Zhao, I. J. Paredes, A. Sahu, and D. -K. Ko, *ACS Appl. Nano Mater.*, **2**, 1631-1636 (2019).
11. A. Sahu, D. Braga, O. Waser, M. S. Kang, D. Deng, and D. J. Norris, *Nano Lett.*, **14**, 115-121 (2014)
12. M. Park, D. Choi, Y. Choi, H. –B. Shin, and K. S. Jeong, *ACS Photonics*, **5**, 1907– 1911 (2018).
13. S. Hafiz, M. Scimeca, A. Sahu, and D. -K. Ko, *Nano Convergence*, **6**, 7 (2019).
14. Y. Liu, M. Gibbs, J. Puthussery, T. Gaik, R. Ihly, H. W. Hillhouse, and M. Law, *Nano Lett.*, **10**, 1960-1969 (2010).